

Trifluoromethylation of a well-defined square-planar Aryl-NiII complex involving NiIII/CF₃ and NiIV–CF₃ intermediate species

ROVIRA, Mireia, ROLDÁN-GÓMEZ, Steven, MARTIN-DIACONESCU, Vlad, WHITEOAK, Christopher <<http://orcid.org/0000-0003-1501-5582>>, COMPANY, Anna, LUIS, Josep and RIBAS, Xavi

Available from Sheffield Hallam University Research Archive (SHURA) at:

<https://shura.shu.ac.uk/16508/>

This document is the Accepted Version [AM]

Citation:

ROVIRA, Mireia, ROLDÁN-GÓMEZ, Steven, MARTIN-DIACONESCU, Vlad, WHITEOAK, Christopher, COMPANY, Anna, LUIS, Josep and RIBAS, Xavi (2017). Trifluoromethylation of a well-defined square-planar Aryl-NiII complex involving NiIII/CF₃ and NiIV–CF₃ intermediate species. *Chemistry - A European Journal*, 23 (48), 11662-11668. [Article]

Copyright and re-use policy

See <http://shura.shu.ac.uk/information.html>

Trifluoromethylation of a well-defined square planar aryl-Ni^{II} complex involving Ni^{III}/CF₃• and Ni^{IV}-CF₃ intermediate species

Mireia Rovira,^{[a]†} Steven Roldán-Gómez,^{[a]†} Vlad Martin-Diaconescu,^[a] Christopher J. Whiteoak,^[a,b] Anna Company,^[a] Josep M. Luis*,^[a] Xavi Ribas*^[a]

Abstract: Ni-mediated trifluoromethylation of an aryl-Br bond in model macrocyclic ligands, **L_n-Br**, has been thoroughly studied, starting with an oxidative addition at Ni⁰ to obtain well-defined aryl-Ni^{II}-Br complexes (**[L_n-Ni^{II}Br]**). Abstraction of the halide with AgX (X = OTf or ClO₄⁻) thereafter provides **[L_n-Ni^{II}](OTf)**. The nitrate analogue has been obtained through a direct C-H activation of an aryl-H bond using Ni^{II} salts, and this route has been studied by XAS. Crystallographic (XRD) and XAS characterization has shown a tight macrocyclic coordination in the aryl-Ni^{II}

complex, which may hamper their direct reaction with nucleophiles. On the contrary, enhanced reactivity is observed with oxidants, and the reaction of **[L_n-Ni^{II}](OTf)** with CF₃⁺ sources afforded **L_n-CF₃** products in quantitative yield. A combined experimental and theoretical mechanistic study provides new insights into the operative mechanism for this transformation. Computational analysis indicate the occurrence of an initial Single Electron Transfer (SET) to 5-(trifluoromethyl)dibenzothiophenium triflate (TDTT) furnishing a transient **L₁-Ni^{III}/CF₃•** adduct, which rapidly

recombines to form a **[L₁-Ni^{IV}-CF₃](X)₂** intermediate species. A final facile reductive elimination affords **L₁-CF₃**. The well-defined square-planar model system here studied permits development of the fundamental knowledge on the rich redox chemistry of nickel, which is sought to facilitate the development of new Ni-based trifluoromethylation methodologies.

Keywords: nickel(IV) • trifluoromethylation • mechanisms • single electron transfer • density functional calculations

Introduction

Tremendous efforts have been directed towards the development of new trifluoromethylating methodologies,^[1] since the CF₃ group can dramatically influence the solubility and stability properties of many pharmaceuticals and agrochemicals. Whilst the vast majority of these transformations use Pd-based catalysts,^[1b, 2] interest is now being directed towards the development of new catalytic protocols using cheaper first-row transition metals such as nickel. The vast majority of C-C and C-Heteroatom coupling reactions catalyzed by nickel typically involve Ni⁰/Ni^I/Ni^{II}/Ni^{III} species in their proposed catalytic pathways,^[3] involving 1e⁻ and 2e⁻ redox steps.^[3a, c, 4] More recently, Ni^{IV} intermediate species have been proposed in transformations involving the Ni^{II}/Ni^{IV} redox couple,^[5] although well-characterized species have only been reported using model substrates designed for octahedral environments.^[6] Such recent studies, in parallel with the development of Pd^{II}/Pd^{IV} catalytic

cycles,^[2b, 7] have sparked interest in high-valent Ni^{IV} organometallic species in new catalytic protocols.

High-valent organometallic Ni complexes have been persistently proposed as putative intermediate species in catalysis, but it was not until 2014 and 2016 that Mirica and co-workers reported the isolation of an octahedral Ni^{III}-dialkyl complex that provided an opportunity to directly probe the involvement of organometallic Ni^{III} and Ni^{IV} species in C-C bond formation cross coupling reactions.^[5b, 8] In 2015, Sanford and co-workers pioneered the isolation of octahedral Ni^{IV} complexes utilizing tris-(2-pyridyl)methane and tris-(pyrazolyl)borate ligand scaffolds, capable of effecting reductive elimination to form C-X bonds (X = O, S, N) and of particular interest, aryl-CF₃ (Scheme 1).^[5a, 9] Sanford's group previously investigated the reactivity of square-planar aryl-Ni^{II} complexes with two electron oxidants, and aryl-Ni^{III}-Br species were proposed as intermediate towards the formation of the aryl-Br final products.^[10]

The extremely rich redox chemistry of Ni complexes demands a deep mechanistic understanding of these processes in order to gain predictability in the development of new Ni-based trifluoromethylation methodologies. Moreover, it is of general interest to gain more mechanistic knowledge about the ability of this metal to form reactive high-valent Ni intermediates in atypical non-octahedral environments. With this idea in mind, we have designed and synthesized an organometallic square-planar aryl-Ni^{II} model system that would enable the stabilization of high valent nickel species. Furthermore, a thorough experimental and theoretical mechanistic study on electrophilic trifluoromethylation of square planar aryl-Ni^{II} species has been performed.

[a] Dr. Mireia Rovira, Mr. Steven Roldán-Gómez, Dr. Vlad Martin-Diaconescu, Dr. Christopher J. Whiteoak, Dr. Josep M. Luis and Dr. Xavi Ribas

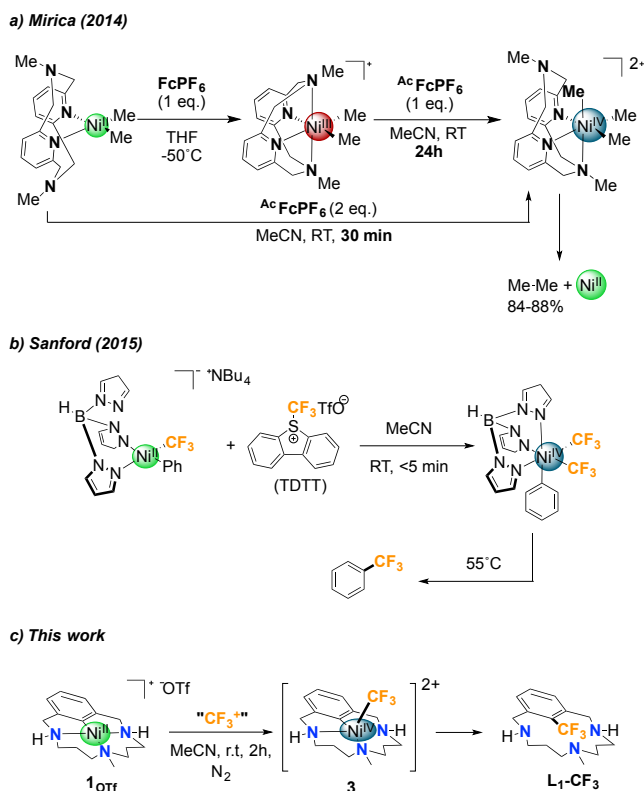
Institut de Química Computacional i Catàlisi (IQCC) and Departament de Química, Universitat de Girona Campus Montilivi, Facultat Ciències, E17071 Girona (Catalonia, Spain), Fax: (+34-972418150)

E-mail: xavi.ribas@udg.edu, josepm.luis@udg.edu

† These authors contributed equally to this work

[b] Current address:

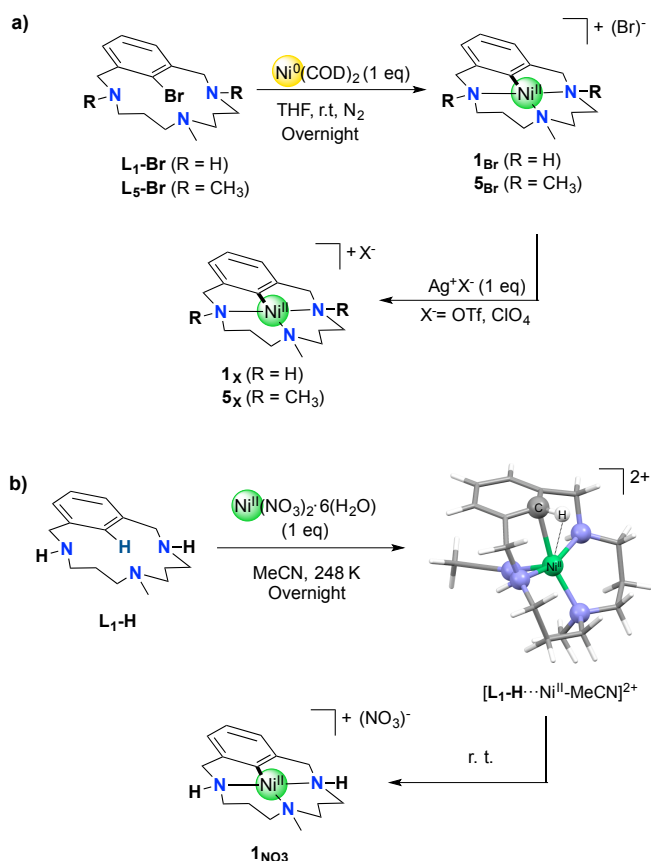
Biomolecular Sciences Research Centre, Faculty of Health and Wellbeing, Sheffield Hallam University, City Campus, Sheffield S1 1WB, England



Scheme 1. (a) Ni^{III} and Ni^{IV}-dialkyl compounds reported by Mirica and co-workers, (b) Ni^{IV} species reported by Sanford and co-workers and (c) the system studied in this work.

Results and Discussion

Organometallic aryl-Ni^{II} complexes [L_n-Ni^{II}](X) (n = 1 or 5, X = OTf⁻, ClO₄⁻ or NO₃⁻) (**1**_{OTf}, **1**_{ClO4}, **1**_{NO3} and **5**_{OTf}) were obtained following two distinct procedures: (a) oxidative addition of L₁-Br to Ni⁰(COD)₂ in THF at room temperature (RT), followed by treatment with AgX (X = ClO₄⁻, OTf⁻), or (b) through direct C-H activation of L₁-H with Ni^{II}(NO₃)₂ (Scheme 2).^[11] The synthesis of complex [L₁-Ni^{II}](X) (**1**_X) through C_{sp2}-H activation of L₁-H was optimized by using Ni^{II}(NO₃)₂·6H₂O as Ni source in MeCN at RT, affording the desired organometallic compound in 55% yield. The addition of soft bases such as acetate did not improve yields (Table S1). All these compounds present diamagnetic NMR spectra as expected for square-planar Ni^{II} complexes.



Scheme 2. Synthesis of the organometallic aryl-Ni^{II} complexes (**1**_{OTf}, **1**_{NO3} and **5**_{OTf}) via (a) oxidative addition at Ni⁰ and (b) direct C-H activation by Ni^{II} (DFT optimized structure of the proposed intermediate, [L₁-H···Ni^{II}-MeCN]²⁺, is shown).

Upon reaction of L₁-H and Ni^{II} salt at low T (248 K) a paramagnetic [L₁-H···Ni^{II}]²⁺ species was obtained. The geometry at the Ni^{II} center and the interaction with the C-H bond was further studied by XAS (Figure 1). XANES and EXAFS analysis point to a most probable trigonal bipyramidal geometry at the metal having 4 N/O scatters at an average distance of 2.09 Å (~ 2.09 Å from DFT) and a C_{aryl} scattering atom at 2.29 Å (~2.39 Å from DFT, see Scheme 2b and Supporting Information). This is in agreement with the complex bearing a coordinated acetonitrile, and consistent with a previously published DFT structure of an analogue complex.^[11]

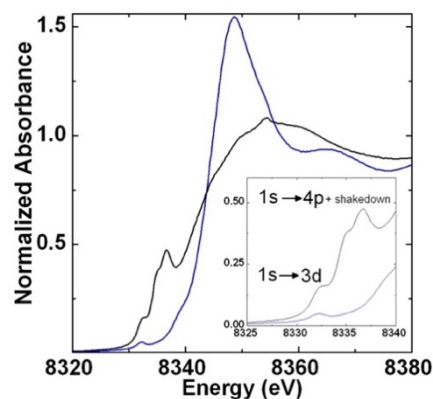


Figure 1. XANES spectra of [L₁-H···Ni^{II}]²⁺ (blue) and **1**_{NO3} in solution (black); Inset: expansion of the pre-edge region.

No C_{sp2}-H activation was observed for L₅-H (macrocyclic model arene substrate bearing N-Me tertiary amines), even in the presence of several bases, or changing the Ni^{II} source, solvent or temperature (Table S2). The corresponding organometallic aryl-Ni^{II} complex [L₅-

$\text{Ni}^{\text{II}}[\text{OTf}]$ ($\mathbf{5}_{\text{OTf}}$) could only be prepared by the oxidative addition using $\text{Ni}^0(\text{COD})_2$ and $\mathbf{L}_5\text{-Br}$ (Scheme 2a). The latter results point towards a key participation of the macrocyclic secondary amines for the $\text{C}_{\text{sp}^2}\text{-H}$ activation process.

On the other hand, compounds $\mathbf{1}_{\text{ClO}_4}$, $\mathbf{1}_{\text{NO}_3}$ and $\mathbf{5}_{\text{OTf}}$ have been crystallographically characterized (Figure 2 and Figure S1-S3), all three displaying a square planar geometry around the Ni^{II} center, which is coordinated to three amines and an aryl moiety. $\text{Ni}^{\text{II}}\text{-C}$ bond distances are found in the range of 1.83-1.84 Å, and $\text{Ni}^{\text{II}}\text{-N}$ in the range of 1.95-2.06 Å. The $\text{Ni}^{\text{II}}\text{-C}$ bond is significantly shorter than analogous macrocyclic aryl- Ni^{II} species using azacalix[1]arene[3]pyridine ligand scaffolds (1.88 Å).^[12] Indeed, the aryl- Ni^{II} bond distances of $\mathbf{1}_X$ are amongst the shortest reported^[11, 13] in the Cambridge Crystallographic Database (typically larger than 1.89 Å).^[6d, 14] The larger $\text{Ni}^{\text{II}}\text{-N}$ bonds for the *trans* coordinated tertiary amine for all three structures arises from the stronger *trans* effect of the aryl moiety. To further explore the coordination environment of the metal center in $\mathbf{1}_{\text{NO}_3}$, XAS at the Ni K-edge was applied as a direct probe of the electronic structure for a solution sample of $\mathbf{1}_{\text{NO}_3}$. EXAFS analysis is consistent with the crystal structure and show the presence of four coordinate complexes having a short Ni-C bond of ~ 1.83 Å with 3 nitrogen scattering atoms in the ~ 1.97 Å range (Figure S8 and Table S6). XANES spectra of a solution sample of $\mathbf{1}_{\text{NO}_3}$ (Figure S7) exhibits a well-resolved and intense pre-edge at 8332.3 eV from $1s \rightarrow 3d$ pre-edge transitions, indicative of a Ni^{II} center with a rising shoulder having two well resolved features at 8334.8 eV and 8336.7 eV. Interestingly, square planar complexes having a centrosymmetric coordination environment are expected to have weak pre-edge intensities of below 0.02 normalized intensity units as exemplified by the spectra of $[\text{Ni}(\text{cyclam})](\text{ClO}_4)_2$.^[15] This is due to the dipole forbidden nature of the $1s \rightarrow 3d$ pre-edge transitions which can only gain intensity through p-d mixing, a process not favored in square planar geometry.^[16] However, the pre-edge of $\mathbf{1}_{\text{NO}_3}$ having an intensity of ~ 0.3 units is similar to the well resolved pre-edge of a previously reported square planar Ni^{II} complex, $[(\text{bpy})\text{Ni}(\text{Mes})\text{Cl}]$, having a $\text{Ni-C}_{\text{aryl}}$ bond of 1.94 Å.^[17] This can be explained by the highly covalent nature of the Ni-C bond, which facilitates p-d mixing through a configuration interaction model, as previously described.^[18] Furthermore, the strength of the $\text{Ni-C}_{\text{aryl}}$ interaction in $\mathbf{1}_{\text{NO}_3}$ is further highlighted by the lower energy of the features due to $1s \rightarrow 4p + \text{shake-down}$ contributions which occur ~ 2 eV lower in energy than in either the previously reported $[(\text{bpy})\text{Ni}(\text{Mes})\text{Cl}]$ complex having a $\text{Ni-C}_{\text{aryl}}$ bond of 1.94 Å or the $[\text{Ni}(\text{cyclam})](\text{ClO}_4)_2$ analogue having no Ni-C bond.^[19]

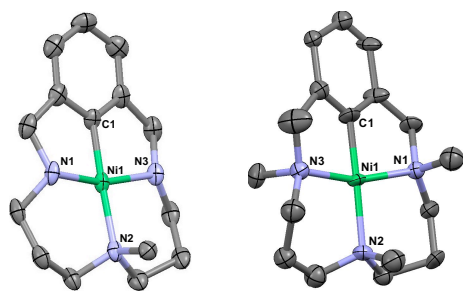


Figure 2. X-Ray crystal structures of $\mathbf{1}_{\text{ClO}_4}$ (left) and $\mathbf{5}_{\text{OTf}}$ (right) at 50% probability level. H atoms and counter anions omitted for clarity. Selected bond distances [Å] and angles [°] for $\mathbf{1}_{\text{ClO}_4}$: Ni(1)-C(1) 1.840(4), Ni(1)-N(3) 1.953(3), Ni(1)-N(1) 1.955(3), Ni(1)-N(2) 2.032(4); C(1)-Ni(1)-N(3) 83.33(18), C(1)-Ni(1)-N(1) 83.68(18), N(3)-Ni(1)-N(1) 164.53(16), C(1)-Ni(1)-N(2) 176.15(16), N(3)-Ni(1)-N(2) 96.68(15), N(1)-Ni(1)-N(2) 95.71(16). Selected bond distances [Å] and angles [°] for $\mathbf{5}_{\text{OTf}}$: Ni(1)-C(1) 1.838(7), Ni(1)-N(3) 1.98(3), Ni(1)-N(1) 1.94(3), Ni(1)-N(2) 2.062(6); C(1)-Ni(1)-N(3) 80.6(11), C(1)-Ni(1)-N(1) 84.2(8), N(3)-Ni(1)-N(1) 163.0(13), C(1)-Ni(1)-N(2) 178.3(10), N(3)-Ni(1)-N(2) 98.9(10), N(1)-Ni(1)-N(2) 96.5(8).

Once the organometallic aryl- Ni^{II} complexes had been fully characterized, we turned our attention towards their reactivity with a range of nucleophiles, such as phenols, boronic acids, and activated methylene compounds amongst others. Unfortunately, no reactivity

was observed using these compounds as coupling partners, indicating the high stability of the aryl- Ni^{II} species. This is in contrast to the analogous macrocyclic aryl- Ni^{II} species using azacalix[1]arene[3]pyridine ligand scaffolds, which readily react with nucleophiles such as phenols, sodium azide and KBr .^[12] The significantly shorter $\text{Ni}^{\text{II}}\text{-C}$ bond of $\mathbf{1}_X$ (1.83-1.84 Å compared to 1.88 Å) suggests a stronger bond due to the tighter macrocyclic coordination compared to the complexes reported by Wang and coworkers, precluding reductive elimination.

The lack of reactivity towards nucleophiles suggested that the rigidity imposed by the macrocyclic environment enforces the superior stability of $\mathbf{1}_X$. At this point we hypothesized that the system may only undergo reactivity provided the Ni^{II} center is further oxidized, and the highly donating macrocyclic ligand platform might allow the access to a high-valent nickel species.^[20] Interestingly, the accessibility to the Ni^{III} oxidation state within the square-planar platforms is clearly visible in the CV spectrum of $\mathbf{1}_{\text{OTf}}$ and $\mathbf{5}_{\text{OTf}}$ showing quasi-reversible $1e^-$ redox couples centered at $E_{1/2} = 0.066$ V and 0.227 V, respectively (vs Ag/AgNO_3) (Figure 3). However, all attempts to react $\mathbf{1}_{\text{OTf}}$ with MeOH as nucleophile (and solvent) in the presence of different $1e^-$ oxidants (Fc^+ , nitrosonium cation (NOSbF_6)), yielded very complex mixtures of side products involving the oxidation of the amine-based ligands to imines, as well as hydrogenation of the aryl moiety to the arene. Similarly, complex mixtures were obtained when malononitrile (active methylene), *p*-methoxyphenol and sodium cyanide were used as nucleophiles. Therefore, albeit generating a much more reactive species when $1e^-$ oxidants are present, we have not been able to control this enhanced reactivity to provide a clean Ni^{III} reductive elimination with the nucleophile. The uncontrolled side reactions of *in situ* generated Ni^{I} species has been discussed very recently by Sanford and coworkers.^[21] Since Ni^{IV} species were reported to undergo reductive elimination with nucleophiles,^[5, 9] we tested $2e^-$ oxidants such as F^+ reagents (*N*-fluoro-2,4,6-trimethylpyridinium triflate (NFTPT), Selectfluor®),^[22] but again multiple decomposition pathways occurred.

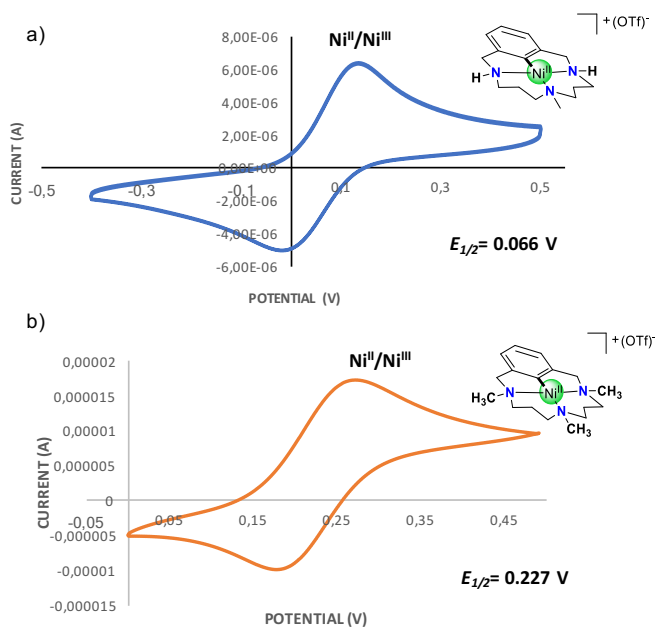
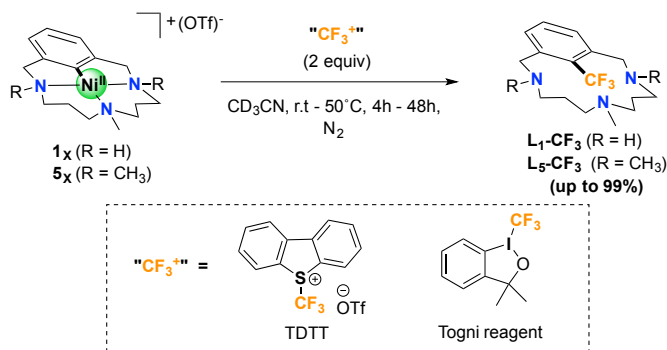


Figure 3. Cyclic Voltammograms of complexes a) $\mathbf{1}_{\text{OTf}}$ (0.5 mM) and b) $\mathbf{5}_{\text{OTf}}$ (1 mM). Conditions: $[\text{n-Bu}_4\text{NPF}_6] = 0.1$ M, CH_3CN , 298 K, scan rate = 0.1 V/s, using non-aqueous Ag/AgNO_3 reference electrode.

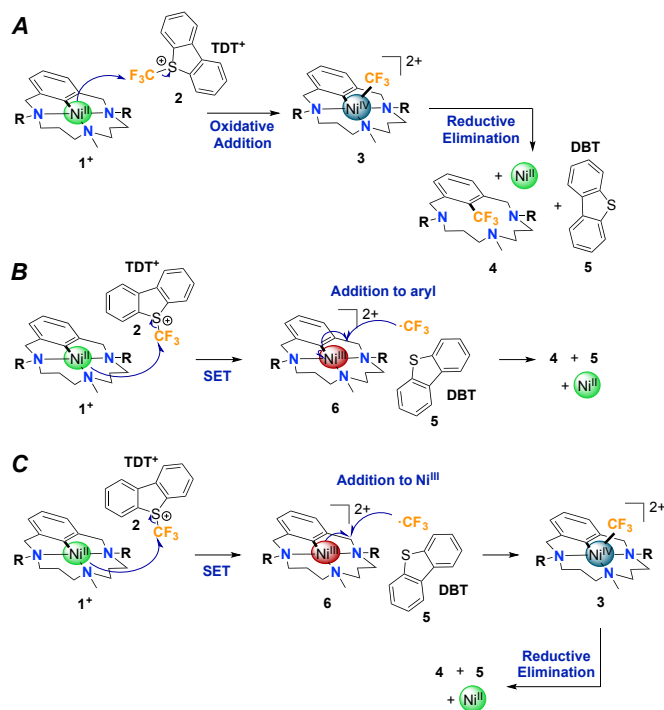
Strikingly, reaction of 1_{OTf} and 5_{OTf} complexes with CF_3^+ sources (5-(trifluoromethyl)dibenzothiophenium trifluoromethanesulfonate (TDTT), 3,3-Dimethyl-1-(trifluoromethyl)-1,2-benziodoxole (Togni reagent)) afforded the quantitative formation of $\text{L}_1\text{-CF}_3$ and $\text{L}_5\text{-CF}_3$ products. Reaction of 1_{OTf} with 2.0 equiv. of TDTT in CD_3CN at room temperature afforded a 99% yield of $\text{L}_1\text{-CF}_3$ in less than 4 hours. When the Togni reagent was used, quantitative trifluoromethylation was also observed, albeit in 12 hours. On the other hand, the reaction of 5_{OTf} with both trifluoromethylating agents required higher temperatures (70°C) and longer reaction times (48 hours) to attain high yields (> 95%, Scheme 3).



Scheme 3. Reactivity of 1_{OTf} and 5_{OTf} in the presence of widely used CF_3^+ oxidants.

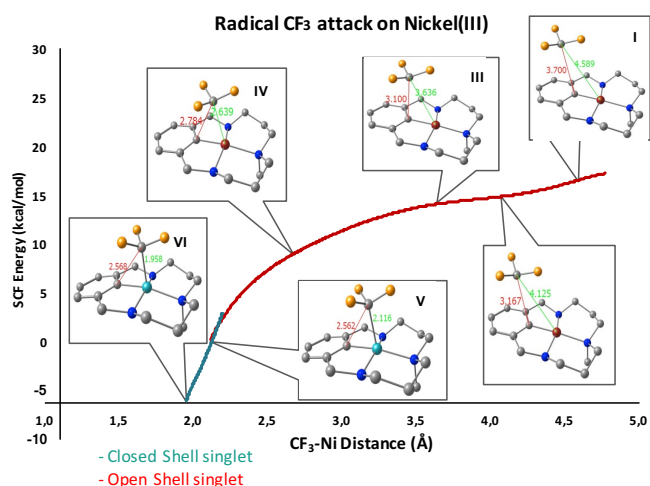
The trifluoromethylated product is likely generated via reductive elimination from a Ni^{IV} intermediate species, similarly to the work reported by Sanford and co-workers.^[9] The slower reactivity observed with 5_{OTf} suggests a lower stability of the high oxidation state on the metal when tertiary amines are used.^[23]

However, the putative aryl- Ni^{IV} intermediated species could not be detected by ^1H NMR spectroscopy even at -40°C, suggesting that this putative intermediate is highly reactive (Figure S6). Therefore, DFT calculations at B3LYP-GD3BJ/cc-pVTZ//B3LYP-GD3BJ/TZPV level (see Experimental section below for more computational details) were employed to further elucidate the reaction mechanism. Based on recent literature concerning Ni complexes and their reactivity, we initially suggested two different pathways (Scheme 4, mechanism **A** and **B**). The first proposal (**A**) was an oxidative-addition step followed by a reductive-elimination step (Figure S10). The second proposal (**B**) involved an initial Single Electron Transfer (SET) followed by a direct radical $\text{CF}_3\cdot$ addition to the aryl group.



Scheme 4. The three proposed mechanisms, **A**, **B** and **C**. Mechanism **A** implies the transfer or flow of two electrons during the reaction (oxidative-addition-like step) followed by a reductive-elimination step; **B** can be described as Single Electron Transfer (SET) followed by a direct radical $\text{CF}_3\cdot$ addition on the aryl group. **C** contains the first step of **B** and the last step of **A**, and then can be considered a combination of **A** and **B**.

Mechanism **A** involved an energetically demanding transition state for the S- CF_3 bond breaking and formal CF_3^+ oxidative addition at the aryl- Ni^{II} cation 1^+ (34.0 kcal/mol) (Figure S10). Different approaches of the CF_3 moiety ($\text{S}_{\text{N}}2$ -like and lateral) were explored but in all cases the oxidative addition barrier was too high (34.0 kcal/mol for the former and 43.7 kcal/mol for the latter). Therefore, we directed our attention towards an initial SET step to form an aryl- Ni^{III} species and a $\text{CF}_3\cdot$ radical (mechanism **B**). The value of the SET barrier calculated using the Marcus theory^[24] (See section 6.1 of the Supporting Information) was low enough (18.0 kcal/mol) to allow the formation of the transient aryl- $\text{Ni}^{\text{III}}/\text{CF}_3\cdot$ adduct (**6**). Strikingly, the IRC calculations used to explore the potential energy surface on the vicinities of the aryl- CF_3 bond distance, show no direct recombination between the radical and the aryl moiety, even if the $\text{CF}_3\cdot$ radical was placed on top of the aryl moiety. On the contrary, the system systematically evolved to a barrierless reaction of the $\text{CF}_3\cdot$ radical and the Ni^{III} center (Scheme 5 and Figure S11) to form the aryl- $\text{Ni}^{\text{IV}}\text{-CF}_3$ intermediate (-0.7 kcal/mol), which then underwent facile reductive elimination to form $\text{L}_1\text{-CF}_3$, with a free energy barrier of only 7.8 kcal/mol. Thus, we have found a more-favorable third possibility (mechanism **C**) that can be seen as a combination of mechanisms **A** and **B** (Scheme 4c and Figure 4). Indeed, mechanism **C** explains why the experimental stabilization of highly oxidized intermediates is hampered. The feasibility of the SET step is in line with the Cyclic Voltammetry experiments, easily accessing to Ni^{III} ($E_{1/2} = 0.066$ V for 1_{OTf} and -0.63 V for TDTT (vs Ag/AgNO_3)).^[25] In fact, the ΔG° obtained (16.0 kcal mol⁻¹) from the standard cell potential ($E^\circ_{\text{cell}} = -0.70$ V) closely matches the DFT thermodynamic energy difference between 1^+ and the aryl- Ni^{III} species obtained by SET (15.2 kcal mol⁻¹). The ground spin state of all the compounds involved in the three studied mechanisms are either closed-shell or open-shell singlet.



Scheme 5. Energy profile computed at B3LYP-GD3BJ/TZPV level and snapshots sequence of the CF₃· attack of the Ni^{III} to generate Ni^{IV}. The plot shows the electronic energy profile of the barrierless approach of the radical to the Ni^{III}. The spin density allowed us to locate the bond distance at which the Ni^{IV}-CF₃ can be initially formed (no spin density on the CF₃). Atomic color code: Ni^{III} in dark red, Ni^{IV} in light blue.

The lifetime of the CF₃· radical generated was evaluated by conducting the trifluoromethylation reaction of **1**_{OTf} and **5**_{OTf} in the presence of the spin trap N-tert-butyl- α -phenylnitrone (PBN). The yield of the desired product was maintained and no decomposition of the radical trap was observed. This is in line with the DFT study, i.e. the transient aryl-Ni^{III}/CF₃· adduct (**6**) has a very short lifetime since the CF₃· radical attack to the Ni^{III} complex is barrierless (Figure 4).

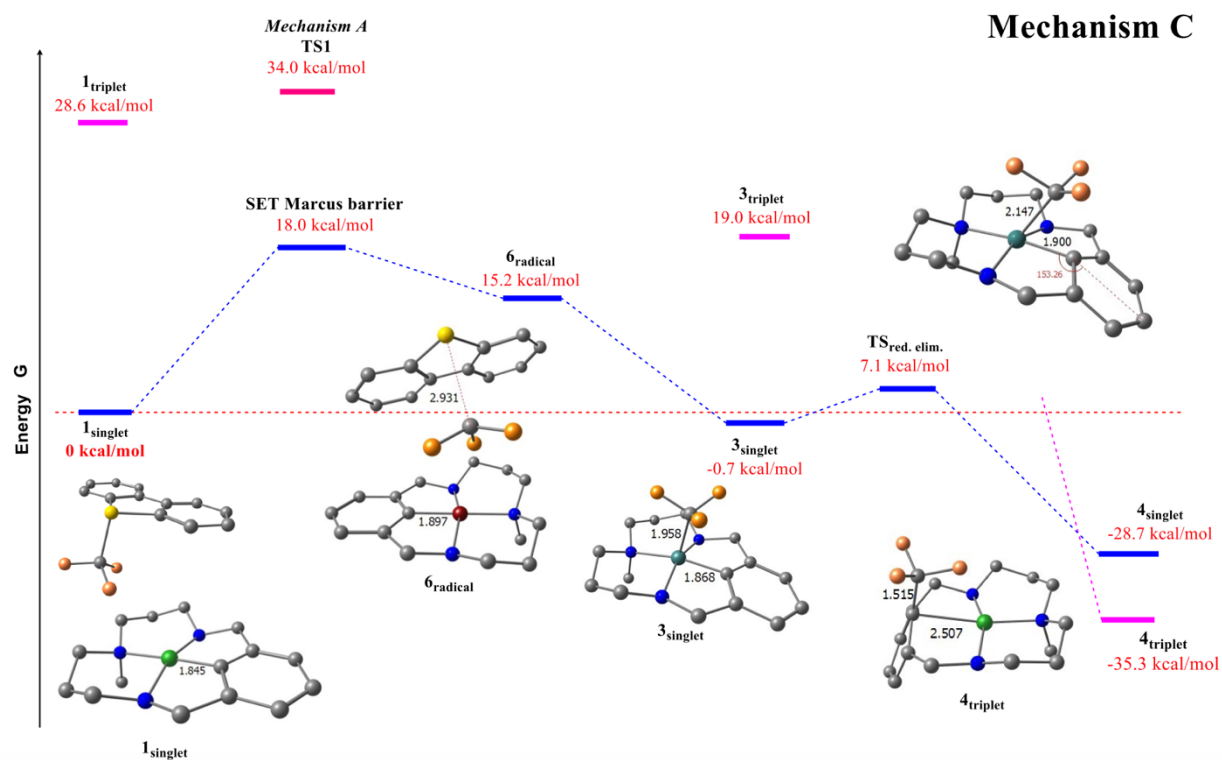


Figure 4. Free Energy profile for the Mechanism C. Free energy values were calculated at (B3LYP-GD3BJ/cc-pVTZ//B3LYP-GD3BJ/TZPV). The blue profiles correspond to most stable open or close shell singlet states, while the triplet states are represented by the fuchsia lines. The determining-step barrier free energy of the mechanism A (TS1, magenta color) is depicted to contrast with the value of the single electron transfer Marcus barrier. The zero Gibbs free energy value of the profile correspond to the free energies of reactants at infinite distance. Color code: N blue, F orange, S yellow, Ni^{II} green, Ni^{III} dark red, Ni^{IV} light blue.

Conclusions

In conclusion, we have described the synthesis and full characterization of well-defined organometallic aryl-Ni^{II} complexes using macrocyclic model systems (**1_X** and **5_{OTf}**), which can be obtained by either oxidative addition at Ni⁰ or Ni^{II} C-H activation. These macrocyclic aryl-Ni^{II} complexes show very short Ni-C bond lengths (1.82 Å) and under the conditions trialed in this study do not react with nucleophiles. However, we have demonstrated their reactivity in the presence of electrophilic CF₃⁺ sources, obtaining quantitative yields of the trifluoromethylated products **L₁-CF₃** and **L₅-CF₃** under mild conditions. Furthermore, experimental and theoretical mechanistic investigations supported a feasible SET step followed by CF₃[·] radical and aryl-Ni^{III} recombination to form an aryl-Ni^{IV}-CF₃ intermediate, which rapidly reductively eliminates to afford the trifluoromethylated products. These well-defined square-planar model platforms allow stepwise information through the redox chemistry of nickel, thus gaining insight into the geometry-dependent reactivity of multiple oxidation states. These results are sought to facilitate the development of new Ni-based trifluoromethylation methodologies.

Experimental Section

Synthesis of complexes 1_X (X = OTf or ClO₄) and 5_{OTf}. The synthesis of aryl-Ni(II) complex **1_{OTf}** was achieved by reacting the model aryl-halide ligand **L₁-Br** with 1 equiv. of Ni(COD)₂ in dry THF under a N₂ atmosphere overnight, affording [Ni^{II}(L₁)]Br (**1_{Br}**, >98% yield). A counter anion exchange was performed in order to improve the solubility of the complex using 1.0 eq. of AgOTf or AgClO₄. This complex is benchtop stable and has been fully characterized both spectroscopically and crystallographically. Full characterization of the complexes can be found in the Supporting Information.

Synthesis of L₁-CF₃ and L₅-CF₃. A screw cap NMR tube was charged with [Ni^{II}(L₁)](OTf) complex (8 mg, 0.0176 mmol, 1.0 equiv) in 0.3 ml CD₃CN, a solution of 5-(Trifluoromethyl)dibenzothiophenium trifluoromethanesulfonate (TDTT) (14.6 mg, 0.035 mmol, 2.0 eq.) in 0.3 ml CD₃CN was subsequently added at room temperature, and the reaction remained light yellow. In a separate experiment, the hypervalent iodine reagent, 3,3-Dimethyl-1-(trifluoromethyl)-1,2-benziodoxole (12.2 mg, 0.035 mmol, 2.0 eq.) was added to [Ni^{II}(L₁)](OTf) complexes in CD₃CN at room temperature for 12 hours. Under these conditions, the yellow solution turned orange. ¹H NMR spectroscopic analyses of the crude reaction mixtures were consistent with the formation of the trifluoromethylated product in more than 99% of yield. Full characterization of the compounds can be found in the Supporting Information.

Preparation of samples for XAS analysis: A 10 mM solution sample of [L₁-H--Ni^{II}](ClO₄)₂ was prepared in butyronitrile by mixing 1.0 eq. of nickel(II) perchlorate with **L₁-H** and immediately freezing the mixture upon loading into a sample cell. Similarly, a 10mM solution of the **1_{NO₃}** was formed by reacting two eq. of the **L₁-H** with 1 eq. of Ni(NO₃)₂ in acetonitrile. The reaction was stirred overnight and then filtered.

Computational details: Gaussian 09 program^[26] was used to perform all DFT calculations. All Structures were optimized using the functional B3LYP^[27] and the Ahlrichs basis set TZVP,^[28] including the Grimme's empirical dispersion model GD3BJ^[29] and the solvent effect of acetonitrile with the PCM-SMD^[30] model. Also, under the same conditions, frequency calculations were carried out to assign the stationary points as transition states (only with one imaginary vibrational frequency) or intermediates (minima with vibrational frequencies real). The frequency calculations were also used to compute thermal and entropic contributions to the Gibbs free energy of each species. All optimized structures were connected by IRC

calculations. Single point energy calculations with a more flexible basis set (cc-pVTZ)^[31] including also the GD3BJ dispersion correction and PCM-SMD solvent correction were performed to obtain better energy estimates. Finally, the correction due to change of conventional 1 atm standard state for gas-phase calculations to a standard-state gas-phase concentration of 1M (except for acetonitrile which is considered at its liquid concentration) was included in all the computed free energies.

XAS experiments details: Solution samples of [L₁-H--Ni^{II}]⁺² and **1_{NO₃}** were run on the XAS beamline at Elettra Sincrotrone Trieste equipped with a Si(111) double crystal monochromator. Solution data was collected in fluorescence mode and samples were kept at ~90 K using a liquid nitrogen finger dewar. Solid samples of **1_{NO₃}** and **1_{ClO₄}** were diluted in boron nitride and were run at the ALBA synchrotron, CLAESS beamline, equipped with a Si(111) double crystal monochromator. A liquid nitrogen flow cryostat was again used to maintain samples at liquid nitrogen temperatures and data was collected in transmission mode.

More details of the XAS spectroscopy experiments and DFT calculations can be found in the Supporting Information.

Crystallographic data for compounds **1_{ClO₄}** (CCDC-1526515), **1_{NO₃}** (CCDC-1526514) and **5_{OTf}** (CCDC-1526516) can be obtained free of charge from the Cambridge Crystallographic Data Centre via www.ccdc.cam.ac.uk/data_request/cif.

Acknowledgements

This work was supported by grants from the European Research Council (Starting Grant Project ERC-2011-StG-277801), the Spanish MICINN (CTQ2016-77989-P and CTQ2014-52525-P), the Catalan DIUE of the Generalitat de Catalunya (2014SGR862 and 2014SGR931). X.R. thanks an ICREA-Acadèmia award. We thank STR from UdG for technical support. XAS experiments were in part performed at CLAESS beamline at ALBA Synchrotron with the collaboration of ALBA staff. X-ray absorption data was also collected at the Elettra facility XAFS beamline and we would like to thank Dr. Luca Olivi for his help with experimental setup.

[1] a) T. Furuya, A. S. Kamlet and T. Ritter, *Nature* **2011**, *473*, 470-477; b) E. J. Cho, T. D. Senecal, T. Kinzel, Y. Zhang, D. A. Watson and S. L. Buchwald, *Science* **2010**, *328*, 1679-1681.

[2] a) A. Maleckis and M. S. Sanford, *Organometallics* **2014**, *33*, 2653-2660; b) N. D. Ball, J. B. Gary, Y. Ye and M. S. Sanford, *J. Am. Chem. Soc.* **2011**, *133*, 7577-7584.

[3] a) B. M. Rosen, K. W. Quasdorf, D. A. Wilson, N. Zhang, A.-M. Resmerita, N. K. Garg and V. Percec, *Chem. Rev.* **2011**, *111*, 1346-1416; b) R. Jana, T. P. Pathak and M. S. Sigman, *Chem. Rev.* **2011**, *111*, 1417-1492; c) S. Z. Tasker, E. A. Standley and T. F. Jamison, *Nature* **2014**, *509*, 299-309; d) V. P. Ananikov, *ACS Catal.* **2015**, *5*, 1964-1971; e) C. M. Lavoie, P. M. MacQueen, N. L. Rotta-Loria, R. S. Sawatzky, A. Borzenko, A. J. Chisholm, B. K. V. Hargreaves, R. McDonald, M. J. Ferguson and M. Stradiotto, *Nat. Commun.* **2016**, *7*, 11073.

[4] a) D. A. Everson and D. J. Weix, *J. Org. Chem.* **2014**, *79*, 4793-4798; b) T. T. Tsou and J. K. Kochi, *J. Am. Chem. Soc.* **1978**, *100*, 1634-1635; c) H.-Q. Do, E. R. R. Chandrashekar and G. C. Fu, *J. Am. Chem. Soc.* **2013**, *135*, 16288-16291; d) J. Cornella, J. T. Edwards, T. Qin, S. Kawamura, J. Wang, C.-M. Pan, R. Gianatassio, M. Schmidt, M. D. Eastgate and P. S. Baran, *J. Am. Chem. Soc.* **2016**, *138*, 2174-2177; e) T. Qin, J. Cornella, C. Li, L. R. Malins, J. T. Edwards, S. Kawamura, B. D. Maxwell, M. D. Eastgate and P. S. Baran, *Science* **2016**, *352*, 801-805.

- [5] a) N. M. Camasso and M. S. Sanford, *Science* **2015**, *347*, 1218-1220; b) J. W. Schultz, K. Fuchigami, B. Zheng, N. P. Rath and L. M. Mirica, *J. Am. Chem. Soc.* **2016**, *138*, 12928-12934.
- [6] a) Y. Aihara and N. Chatani, *J. Am. Chem. Soc.* **2014**, *136*, 898-901; b) Y. Aihara and N. Chatani, *J. Am. Chem. Soc.* **2013**, *135*, 5308-5311; c) X. Wu, Y. Zhao and H. Ge, *J. Am. Chem. Soc.* **2014**, *136*, 1789-1792; d) G. E. Martinez, C. Ocampo, Y. J. Park and A. R. Fout, *J. Am. Chem. Soc.* **2016**, *138*, 4290-4293.
- [7] a) T. W. Lyons and M. S. Sanford, *Chem. Rev.* **2010**, *110*, 1147-1169; b) A. J. Hickman and M. S. Sanford, *Nature* **2012**, *484*, 177-185; c) K. Muñoz, *Angew. Chem. Int. Ed.* **2009**, *48*, 9412-9423.
- [8] a) B. Zheng, F. Tang, J. Luo, J. W. Schultz, N. P. Rath and L. M. Mirica, *J. Am. Chem. Soc.* **2014**, *136*, 6499-6504; b) W. Zhou, S. Zheng, J. W. Schultz, N. P. Rath and L. M. Mirica, *J. Am. Chem. Soc.* **2016**, *138*, 5777-5780; c) M. B. Watson, N. P. Rath and L. M. Mirica, *J. Am. Chem. Soc.* **2017**, *139*, 35-38.
- [9] J. R. Bour, N. M. Camasso and M. S. Sanford, *J. Am. Chem. Soc.* **2015**, *137*, 8034-8037.
- [10] a) A. T. Higgs, P. J. Zinn, S. J. Simmons and M. S. Sanford, *Organometallics* **2009**, *28*, 6142-6144; b) A. T. Higgs, P. J. Zinn and M. S. Sanford, *Organometallics* **2010**, *29*, 5446-5449.
- [11] X. Ribas, C. Calle, A. Poater, A. Casitas, L. Gómez, R. Xifra, T. Parella, J. Benet-Buchholz, A. Schweiger, G. Mitrikas, M. Solà, A. Llobet and T. D. P. Stack, *J. Am. Chem. Soc.* **2010**, *132*, 12299-12306.
- [12] C. Yang, W.-D. Wu, L. Zhao and M.-X. Wang, *Organometallics* **2015**, *34*, 5167-5174.
- [13] a) D. M. Grove, G. Van Koten, H. J. C. Ubbels, R. Zoet and A. L. Spek, *Organometallics* **1984**, *3*, 1003-1009; b) J.-P. Cloutier, B. Vabre, B. Mounang-Soumé and D. Zargarian, *Organometallics* **2015**, *34*, 133-145; c) M. Stol, D. J. M. Snelders, M. D. Godbole, R. W. A. Havenith, D. Haddleton, G. Clarkson, M. Lutz, A. L. Spek, G. P. M. van Klink and G. van Koten, *Organometallics* **2007**, *26*, 3985-3994; d) L. A. v. d. Kuil, Y. S. J. Veldhuizen, D. M. Grove, J. W. Zwikker, L. W. Jenneskens, W. Drenth, W. J. J. Smeets, A. L. Spek and G. v. Koten, *Rec. Trav. Chim. Pays-Bas* **1994**, *113*, 267.
- [14] a) N. D. Schley and G. C. Fu, *J. Am. Chem. Soc.* **2014**, *136*, 16588-16593; b) Z. He and Y. Huang, *ACS Catal.* **2016**, *6*, 7814-7823.
- [15] G. J. Colpas, M. J. Maroney, C. Bagyinka, M. Kumar, W. S. Willis, S. L. Suib, N. Baidya and P. K. Mascharak, *Inorg. Chem.* **1991**, *30*, 920-928.
- [16] a) V. Martin-Diaconescu, M. Gennari, B. Gerey, E. Tsui, J. Kanady, R. Tran, J. Pécaut, D. Maganas, V. Krewald, E. Gouré, C. Duboc, J. Yano, T. Agapie, M.-N. Collomb and S. DeBeer, *Inorg. Chem.* **2015**, *54*, 1283-1292; b) T. E. Westre, P. Kennepohl, J. G. DeWitt, B. Hedman, K. O. Hodgson and E. I. Solomon, *J. Am. Chem. Soc.* **1997**, *119*, 6297-6314.
- [17] A. Klein, A. Kaiser, W. Wielandt, F. Belaj, E. Wendel, H. Bertagnolli and S. Zális, *Inorg. Chem.* **2008**, *47*, 11324-11333.
- [18] a) S. DeBeer George, P. Brant and E. I. Solomon, *J. Am. Chem. Soc.* **2005**, *127*, 667-674; b) V. Martin-Diaconescu, K. N. Chacón, M. U. Delgado-Jaime, D. Sokaras, T.-C. Weng, S. DeBeer and N. J. Blackburn, *Inorg. Chem.* **2016**, *55*, 3431-3439.
- [19] R. Sarangi, *Coord. Chem. Rev.* **2013**, *257*, 459-472.
- [20] a) K. Koo and G. L. Hillhouse, *Organometallics* **1995**, *14*, 4421-4423; b) K. Koo and G. L. Hillhouse, *Organometallics* **1996**, *15*, 2669-2671; c) R. Han and G. L. Hillhouse, *J. Am. Chem. Soc.* **1998**, *120*, 7657-7658; d) G. G. Dubinina, W. W. Brennessel, J. L. Miller and D. A. Vicic, *Organometallics* **2008**, *27*, 3933-3938; e) J. Jover, F. M. Miloserdov, J. Benet-Buchholz, V. V. Grushin and F. Maseras, *Organometallics* **2014**, *33*, 6531-6543.
- [21] J. R. Bour, N. M. Camasso, E. A. Meucci, J. W. Kampf, A. J. Canty and M. S. Sanford, *J. Am. Chem. Soc.* **2016**, *138*, 16105-16111.
- [22] H. Lee, J. Börgel and T. Ritter, *Angew. Chem. Int. Ed.* **2017**, DOI: 10.1002/anie.201701552.
- [23] G. Golub, H. Cohen, P. Paoletti, A. Bencini, L. M. Bertini and D. Meyerstein, *J. Am. Chem. Soc.* **1995**, *117*, 8353-8361.
- [24] a) R. A. Marcus, *J. Chem. Phys.* **1956**, *24*, 966-978; b) V. Postils, A. Company, M. Solà, M. Costas and J. M. Luis, *Inorg. Chem.* **2015**, *54*, 8223-8236; c) A. Amini and A. Harriman, *J. Photochem. Photobiol. C: Photochem. Rev.* **2003**, *4*, 155-177.
- [25] S. Mizuta, S. Verhoog, X. Wang, N. Shibata, V. Gouverneur and M. Médebielle, *J. Fluor. Chem.* **2013**, *155*, 124-131.
- [26] M. J. T. Frisch, G. W.; Schlegel, H. B.; Scuseria, G. E.; Robb, M. A.; Cheeseman, J. R.; Scalmani, G.; Barone, V.; Mennucci, B.; Petersson, G. A.; Nakatsuji, H.; Caricato, M.; Li, X.; Hratchian, H. P.; Izmaylov, A. F.; Bloino, J.; Zheng, G.; Sonnenberg, J. L.; Hada, M.; Ehara, M.; Toyota, K.; Fukuda, R.; Hasegawa, J.; Ishida, M.; Nakajima, T.; Honda, Y.; Kitao, O.; Nakai, H.; Vreven, T.; Montgomery, J. A., Jr.; Peralta, J. E.; Ogliaro, F.; Bearpark, M.; Heyd, J. J.; Brothers, E.; Kudin, K. N.; Staroverov, V. N.; Kobayashi, R.; Normand, J.; Raghavachari, K.; Rendell, A.; Burant, J. C.; Iyengar, S. S.; Tomasi, J.; Cossi, M.; Rega, N.; Millam, M. J.; Klene, M.; Knox, J. E.; Cross, J. B.; Bakken, V.; Adamo, C.; Jaramillo, J.; Gomperts, R.; Stratmann, R. E.; Yazyev, O.; Austin, A. J.; Cammi, R.; Pomelli, C.; Ochterski, J. W.; Martin, R. L.; Morokuma, K.; Zakrzewski, V. G.; Voth, G. A.; Salvador, P.; Dannenberg, J. J.; Dapprich, S.; Daniels, A. D.; Farkas, Ö.; Foresman, J. B.; Ortiz, J. V.; Cioslowski, J.; Fox, D. J. in *Gaussian 09, Revision D.01*, Vol. Gaussian Inc., Wallingford CT, **2009**.
- [27] a) A. D. Becke, *J. Chem. Phys.* **1993**, *98*, 1372-1377; b) C. Lee, W. Yang and R. G. Parr, *Phys. Rev. B* **1988**, *37*, 785-789; c) S. H. Vosko, L. Wilk and M. Nusair, *Can. J. Phys.* **1980**, *58*, 1200-1211; d) P. J. Stephens, F. J. Devlin, C. F. Chabalowski and M. J. Frisch, *J. Phys. Chem.* **1994**, *98*, 11623-11627.
- [28] a) A. Schäfer, C. Huber and R. Ahlrichs, *J. Chem. Phys.* **1994**, *100*, 5829-5835; b) A. Schäfer, H. Horn and R. Ahlrichs, *J. Chem. Phys.* **1992**, *97*, 2571-2577.
- [29] S. Grimme, S. Ehrlich and L. Goerigk, *J. Comput. Chem.* **2011**, *32*, 1456-1465.
- [30] A. V. Marenich, C. J. Cramer and D. G. Truhlar, *J. Phys. Chem. B* **2009**, *113*, 6378-6396.
- [31] a) R. A. Kendall, T. H. D. Jr. and R. J. Harrison, *J. Chem. Phys.* **1992**, *96*, 6796-6806; b) E. R. Davidson, *Chem. Phys. Lett.* **1996**, *260*, 514-518.